Streamflow Drought Interpreted Using SWAT Model Simulations of Past and Future Hydrologic Scenarios: Application to Neches and Trinity River Basins, Texas

Dagbegnon Clement Sohoulande Djebou[1]

Abstract: In water resources and environmental management, hydrologic indexes are often valued as decision support tools because of their practical interpretability. This is true with the streamflow drought index (SDI), which is considered to be a relevant tool for assessing the availability of water resources at the watershed level. Hence, the future of freshwater resources at the watershed scale could be better understood by achieving a realistic projection of SDI. This study used a process-based watershed modeling approach to describe a framework for SDI projection. Specifically, the Soil and Water Assessment Tool (SWAT) model was used to simulate distinctly two watersheds located in the state of Texas, the Trinity and the Neches River Basins. The SWAT model was calibrated with monthly streamflow data for the period 1990–1995. The model was subsequently validated with two decades of discharge data (1996–2015). The evaluation of the SWAT performance during the calibration and validation stages showed acceptable values of efficiency criteria for both watersheds (i.e., Nash-Sutcliffe efficiency ranging from 0.56 to 0.65; index of agreement from 0.79 to 0.92). The calibrated model was used to simulate runoff for the future period 2041–2070 using inputs retrieved from a future climate scenario. However, the SDI calculation requires knowledge of the probability distribution of cumulative discharge data. A Kolmogorov-Smirnov's goodness-of-fit analysis was conducted for both observed and simulated cumulative discharges. A lognormal distribution was considered for estimating time series of SDI. For the period 1996–2015, the SDI values recovered from the SWAT simulations matched closely with those derived directly from the observed discharge data ($0.52 \le R^2 \le 0.91$ for the Neches River, and $0.79 \le R^2 \le 0.89$ for the Trinity River). This result demonstrated the capacity of the analytical procedure to capture and project realistically SDI signals. However, analysis of the χ^2 statistic of the SDI patterns for the past and the future periods did not reveal any significant difference. **DOI: 10.1061/(ASCE)HE.1943-5584.0001827.**

Author keywords: Drought index; Soil and Water Assessment Tool (SWAT) model; Streamflow; Watershed; Lognormal distribution; Climate scenario.

Introduction

Drought is a complex phenomenon which generally originates from a low-precipitation period (McKee et al. 1993). Drought is often accompanied with diverse consequences for natural ecosystems and the human society (Vicente-Serrano et al. 2012). Sometimes the consequences of drought can be irreversible and long-lasting (Sohoulande Djebou 2017). For that reason, drought has been intensively investigated in time and space with the purpose of thoroughly understanding the phenomenon (McKee et al. 1993). Unfortunately, the accurate projection of drought occurrence and severity remains a puzzle (Deo et al. 2017; Mishra and Desai 2006). This shortcoming is detrimental for achieving adequate water resources planning in many watersheds.

Over time, different types of drought have been distinguished and given specific attention (McKee et al. 1993; Wilhite and Glantz 1985). Among these types of drought, streamflow drought has specific implications for aquatic ecosystems which are directly affected by the quantitative availability of surface water (Smakhtin 2001). Streamflow drought is a temporary event which occurs when the discharge during a period is below predetermined thresholds given by the probability density function of streamflow (Vicente-Serrano et al. 2012). Thus, the duration of streamflow drought corresponds to the period in which the discharge is below the corresponding thresholds. However, the use of the streamflow drought index (SDI) is more practical for quantifying the severity of this type of drought (Tabari et al. 2013; Nalbantis and Tsakiris 2009). Specifically, the SDI is very informative because it provides scaled values of surface water anomalies at the watershed level. Nevertheless, it is often difficult to project the hydrologic behavior of a watershed, which normally depends on a set of biophysical factors interacting diversely in time and space (Tidwell et al. 2004). However, it is well established that the use of physically based models such as the Soil and Water Assessment Tool (SWAT) has significantly improved the capacity to represent hydrological processes at the watershed scale (Gassman et al. 2014).

The present study evaluated the capacity of the SWAT model to reproduce patterns of streamflow drought at the watershed level. Two watersheds located in the state of Texas were simulated for monthly discharge. The SDI time series derived from observed and simulated discharges of a past period were comparatively

[1]Research Agricultural Engineer, US Dept. of Agriculture–Agricultural Research Service Coastal Plain Soil, Water, and Plant Conservation Research Center, 2611 W. Lucas St., Florence, SC 29501. ORCID: https://orcid.org/0000-0001-8963-869X. Email: clement.sohoulande@ars.usda.gov; sohoulande@yahoo.fr

Note. This manuscript was submitted on November 21, 2017; approved on April 18, 2019; published online on June 27, 2019. Discussion period open until November 27, 2019; separate discussions must be submitted for individual papers. This paper is part of the ***Journal of Hydrologic Engineering***, © ASCE, ISSN 1084-0699.

analyzed to elucidate the SWAT performance at capturing streamflow drought signals. Afterward, an analysis was carried out with the aim of comparing future patterns of SDI with past patterns. The results are reported and the relevance of using SWAT simulations in SDI projection are discussed.

Method

The methodological approach used for this study consisted of two analytical components, SWAT modeling and a streamflow drought analysis. Two watersheds were targeted in the state of Texas, and their related hydrological and spatial data were collected and assessed. The study used three types of data sets: spatial, streamflow, and weather data.

Data and Watersheds

Watersheds and Streamflow Data

The study addressed distinctly the streamflow behavior in two watersheds located in the state of Texas. These watersheds are the Neches River Basin and the Trinity River Basin (Fig. 1). In the United States, the state of Texas is known for facing critical challenges in managing surface water resources. The hydrographs of the cumulative discharge in each of the selected watershed showed strong patterns of high flow volumes alternated with low flow volumes (Fig. 2). The observed sequences were irregular, suggesting complex streamflow anomalies and the need to anticipate water resources concerns. This was the rationale for the selection of the Neches and the Trinity River Basins in this study. These two basins partially share a boundary and they both pertain to the Texas Gulf, which is a shallow regional watershed with a less contrasted topography.

At the watershed level, a stream gauge (i.e., streamflow station) was targeted and the corresponding monthly discharge time series for the period 1990–2015 were retrieved from the USGS database. Hence, in the Trinity River Basin, the stream gauge considered is located at 31.65°N latitude and 95.79°W longitude, and it has the USGS Hydrologic Unit Code (HUC) 12020003. In the Neches River Basin, the stream gauge considered is located at 30.79°N latitude and 94.15°W longitude, and its USGS HUC is 12030201. The estimated drainage area using the SWAT watershed delineator was 19,574 km^2 for the simulated watershed in the Neches River Basin and 33,262 km^2 in the Trinity River Basin. The observed monthly discharge time series of 1990–2015 were used during the calibration and validation stages of the SWAT modeling. Both selected stream gauges had no gaps in their records of monthly streamflow data for the period 1990–2015. During the SWAT simulations, the locations of the stream gauges served as outlets.

Spatial Data

Three categories of spatial data were used. The first category was a 30-m spatial resolution digital elevation model (DEM). The DEM data were retrieved from the National Elevation Dataset (NED), which is released by the USEPA. The second category was the National Land Cover Database (NLCD) 2011, which has a spatial resolution of 30 m and counts 16 classes of land-cover types (Homer et al. 2015). The data were developed and released by the Multi-Resolution Land Characteristics (MRLC) Consortium. The third category was the State Soil Geographic database (STATSGO), which was developed by the National Cooperative

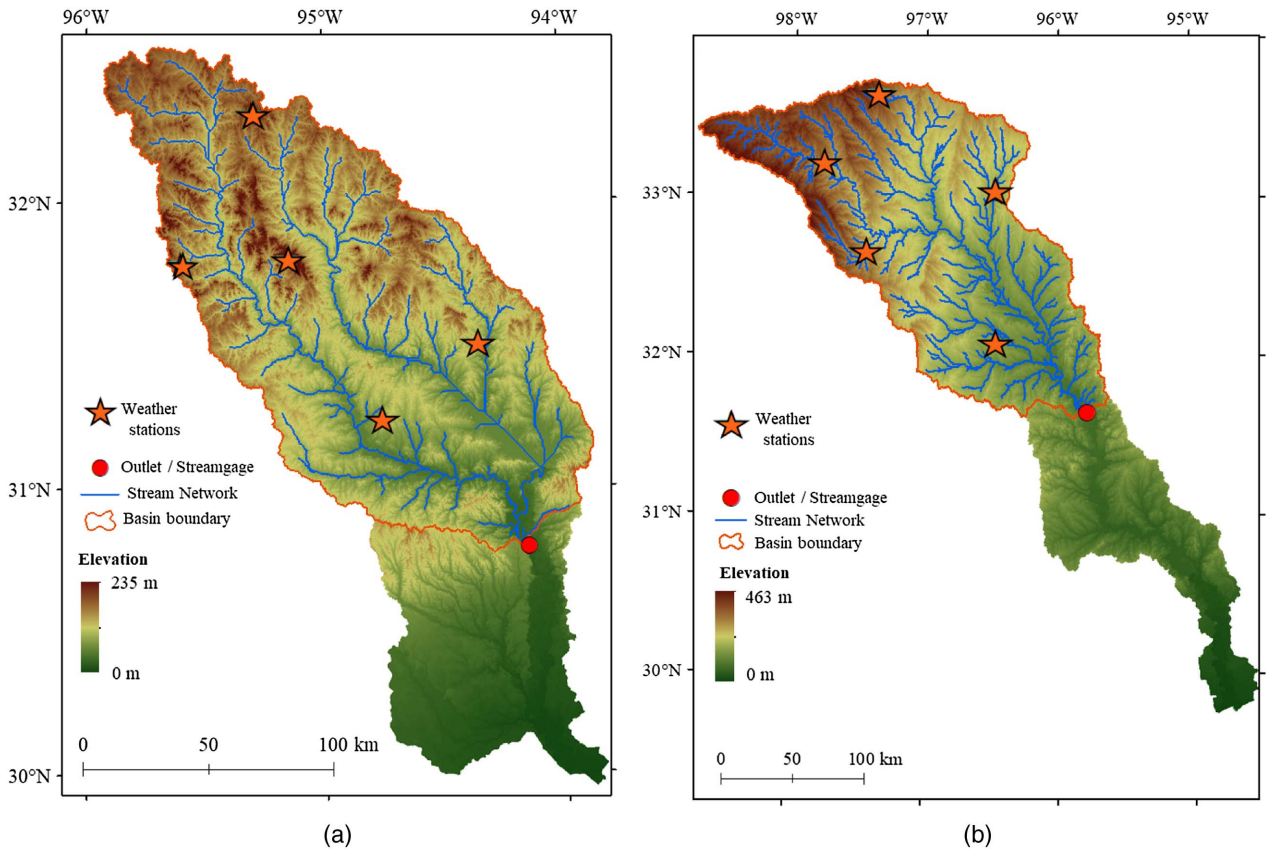

Fig. 1. Delineated watersheds showing locations of the weather stations and the streamflow outlet considered for the SWAT modeling of the (a) Neches River Basin; and (b) Trinity River Basin.

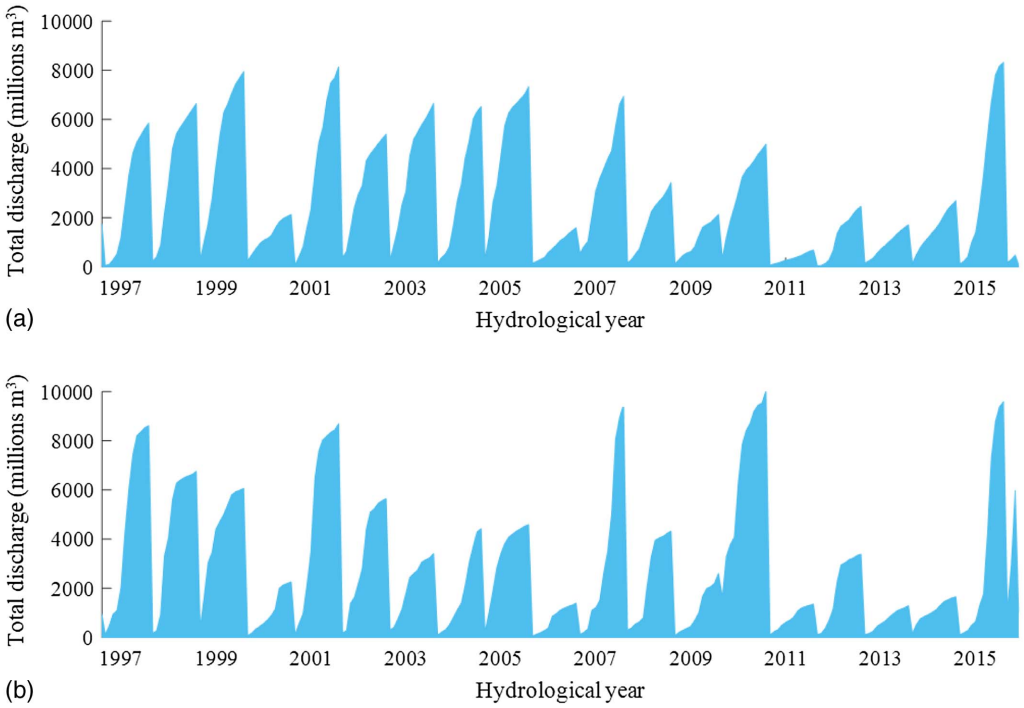

Fig. 2. Hydrographs showing the sequences of cumulative discharges during consecutive hydrologic years from 1996 to 2015 in the (a) Neches River watershed at outlet 30.79° N, 94.15° W; and (b) Trinity River watershed at outlet 31.65° N, 95.79° W. A USGS hydrologic year is a period spanning from October of year Y to September of year $Y + 1$.

Soil Survey of the USDA. The use of the STATSGO soil map data for this study was motivated by the size of the watersheds addressed; the type of simulation (i.e., discharge); and the temporal resolution, which was monthly (Geza and McCray 2008; Wang and Melesse 2006). Indeed, several authors agreed that the STATSGO soil map is appropriate when streamflow is simulated and when the watershed is relatively large (Mukundan et al. 2010; Geza and McCray 2008; Wang and Melesse 2006).

Weather Data

The weather data used in the study consisted of daily time series of precipitation and temperature for past and future time slices (i.e., 1990–2015 and 2041–2070). For the past weather data, five weather stations were selected across each delineated watershed (Fig. 1). For individual weather stations, the historical daily precipitation, and maximum and minimum temperatures for the period 1990–2015 were obtained from the Global Historical Climatology Network (GHCN) database of the NOAA. The geographic locations of these weather stations are presented in Table 1. The selected weather stations had an average 0.2% missing data for daily precipitation and 1.8% missing data for daily maximum and minimum temperatures. During the SWAT simulation, the missing weather data were replaced with values generated by the SWAT's weather generator. Indeed, the SWAT's weather generator is used as default input when a real-time measurement of a variable is missing.

The study used simulated weather data for the future period 2041–2010. These data were developed by the North American Regional Climate Change Assessment (NARCCAP) (Wehner 2013). Specifically, the study used daily precipitation and daily maximum/minimum temperature data of the NARCCAP Regional Climate Model 3 (RCM3). The NARCCAP RCM3 is driven by boundary conditions defined by the Geophysical Fluid Dynamics Laboratory (GFDL) (Mearns et al. 2012). Several authors reported the consistency of the NARCCAP simulations over the conterminous United States (Ahmed et al. 2013; Mearns et al. 2012). The NARCCAP simulation is based on Scenario A2 of the Intergovernmental Panel on Climate Change's Special Report on Emissions (IPCC-SRES), which assumed a world population of 10 billion by 2050 with a projected CO_2 concentration of 575 ppm (Nakicenovic et al. 2000). The NARCCAP RCM3-GFDL simulations are released as gridded time series with a 50-km spatial resolution. However, for the SWAT simulations, the study used the geographic coordinates listed in Table 1, then retained the nearest grids in lieu of the five weather stations of Fig. 1. The NARCCAP future climate simulations are released only for the period 2041–2070, which justified the use of the same time slice for the SWAT simulation of the future period. Several authors used RCM simulations in SWAT modeling, and reported them to be useful for understanding future hydrological patterns at the watershed scale

Table 1. Locations of weather stations used for SWAT modeling

Watershed	Station ID	Latitude (°N)	Longitude (°W)	Elevation (m)
Neches	USW00093987	31.24	94.75	87.8
	USC00411711	31.50	94.35	100.6
	USW00093915	31.78	95.60	141.7
	USC00419207	32.31	95.30	167.6
	USC00417841	31.80	95.15	219.5
Trinity	USC00412019	32.08	96.47	129.5
	USC00415094	33.03	96.48	155.4
	USC00411063	33.21	97.78	234.4
	USC00410691	32.65	97.45	240.8
	USC00416130	33.65	97.37	306.3

Note: Station ID provided by the Global Historical Climatology Network, which is an integrated database for ground-based stations.

(Zabaleta et al. 2014; Gassman et al. 2014). The present study used the historical streamflow and weather data of period 1990–2015 during the stages of calibration (1990–1995) and validation (1996–2015) of the SWAT model. Subsequently, the future weather data were used as inputs during the SWAT simulation of the future period.

SWAT Modeling

ArcSWAT version 2012.10.19 was used to model streamflow in the Neches and the Trinity watersheds. The described spatial and weather data were used as inputs during the modeling. The SWAT modeling procedure consisted of three stages, the calibration (1990–1995), the validation (1996–2015), and the future period simulation (2041–2070).

Model Calibration

Using the observed monthly discharge of the period 1990–1995 as a reference, the SWAT model was manually calibrated for the Neches and Trinity watersheds. The calibration was performed by adjusting the input parameters. According to Vrugt et al. (2008), most of the parameters cannot be inferred through direct observation in the field, but by using an adjustment process. This justifies the relevance of the manual adjustment, but the success of the process depends also on the modeler's ability (Eckhardt and Arnold 2001). In the case of the studied watersheds, the most sensitive parameters were found to be Curve number CN2 and the available soil water content, Soil-AWC. These two parameters were adjusted iteratively, and the operation was repeated several times until acceptable efficiencies were reached. The SWAT model performance was assessed by calculating three different indicators of fitness, the Nash-Sutcliffe efficiency (NSE) [Eq. (1)], the index of agreement d [Eq. (2)], and the RMS error (RMSE) [Eq. (3)] (McCuen et al. 2006; Legates and McCabe 1999; Willmott 1981). The first year, 1990, was considered as a warming period while running the SWAT model. Therefore, the values of the year 1990 were not included in the performance evaluation

$$\text{NSE} = 1 - \frac{\sum_{i=1}^{N} (Q_i - \hat{Q}_i)^2}{\sum_{i=1}^{N} (Q_i - \bar{Q})^2} \tag{1}$$

$$\text{Index of agreement}\,(d) = 1 - \frac{\sum_{i=1}^{N} (Q_i - \hat{Q}_i)^2}{\sum_{i=1}^{N} (|\hat{Q}_i - \bar{Q}| + |Q_i - \bar{Q}|)^2} \tag{2}$$

$$\text{RMSE} = \left[\sum_{i=1}^{N} \frac{(Q_i - \hat{Q}_i)^2}{N}\right]^{0.5} \tag{3}$$

where N = number of months during the simulation period; Q_i and $\hat{Q}_i$ = observed and simulated discharge, respectively, for month i; and $\bar{Q}$ = observed average discharge.

Model Validation and Future Streamflow Simulation

The calibrated SWAT model was used to simulate separately the streamflow for past and future time slices (1996–2015 and 2041–2070). The relatively large period (i.e., 2 decades) used for the validation period was relevant because the study evaluated the SWAT model's capacity to capture streamflow drought signals during a multidecadal time frame and enable a comparison with the future-period SWAT simulations (i.e., 2041–2070). The performance of the model during the validation period was addressed using NSE, d, and RMSE. Following a satisfactory validation stage, the calibrated SWAT model was used in an application for the future period 2041–2070. This step used the daily weather data obtained from the NARCCAP RCM3-GFDL simulations. The simulated streamflow data were subsequently processed, and values of the streamflow drought index were estimated for the entire period 2041–2070.

Streamflow Drought Index

In their effort to characterize streamflow drought, scientists developed a variety of indexes which have practical implications for water resources and environmental management (Tabari et al. 2013; Vicente-Serrano et al. 2012). The present study emphasized the streamflow drought index as reported by Nalbantis and Tsakiris (2009). The SDI is analogous to the standardized precipitation index (SPI) and it has relevant applicability at the watershed scale (Tabari et al. 2013; Nalbantis and Tsakiris 2009). The SDI is probability-based and formulated such that both seasonal and interannual variability of the streamflow are represented (Tabari et al. 2013; Nalbantis and Tsakiris 2009). Nalbantis and Tsakiris (2009) highlighted five categories of streamflow drought: no drought ($0 \le \text{SDI}$), mild ($-1 \le \text{SDI} < 0$), moderate ($-1.5 \le \text{SDI} < -1$), severe ($-2 \le \text{SDI} < -1.5$), and extreme ($\text{SDI} < -2$). The calculation of the SDI involved a consideration of USGS hydrologic year. The USGS hydrologic year, or water year, is defined as the period from October of year Y to September of year $Y + 1$ (Slack and Landwehr 1992). Assuming the USGS hydrological year definition, a time series of monthly streamflow discharge of an n-year period can be defined by a series of discharge $Q_{\tau,\phi}$, where τ denotes the hydrological year and ϕ represents the month within the year (i.e., $\phi = 1$ for October, $\phi = 2$ for November, $\phi = 3$ for December, $\phi = 4$ for January, $\ldots$, $\phi = 12$ for September). The computation of SDI is associated with reference periods of the hydrological year denoted here by θ. Thus $\theta = 1$ for the cumulative period October–December, $\theta = 2$ for October–March, $\theta = 3$ for October–June, and $\theta = 4$ for October–September. For individual hydrologic years, four values of SDI were then calculated in accordance with the reference periods of the hydrological year (i.e., $\theta = 1, 2, 3$, and 4). As a result, the time series of SDI can be addressed separately for each referential period. The computation of SDI requires knowledge of the probability distribution of the cumulative discharge data. Given a time series of discharge $Q_{\tau,\phi}$, a corresponding cumulative discharge $V_{\tau,\theta}$ can be retrieved, and then the $SDI_{\tau,\theta}$ is calculated using

$$\text{SDI}_{\tau,\theta} = \frac{V_{\tau,\theta} - \overline{V_\theta}}{s_\theta} \tag{4}$$

$$\bar{V}_\theta = \sum_{\tau=1}^{n} \frac{V_{\tau,\theta}}{n}; \qquad S_\theta = \sqrt{\sum_{\tau=1}^{n} \frac{(V_{\tau,\theta} - \bar{V}_\theta)^2}{n}} \tag{5}$$

$$V_{\tau,\theta} = \sum_{\phi=1}^{3\theta} Q_{\tau,\phi}; \quad \tau = 1, 2, \ldots, n; \quad \theta = 1, 2, 3, 4; \quad \phi = 1, 2, \ldots, 12 \tag{6}$$

In principle, ϕ in Eq. (6) could be any month of the year (i.e., $\phi = 1, 2, \ldots, 12$). However, for the computation of SDI, this study only considered cumulative periods based on the USGS hydrologic year, which starts from October ($\phi = 1$ = October). The use of these indexing equations [Eqs. (4)–(6)] is adequate when the cumulative discharge probability distribution is normal or transformed into a normal distribution (Ben-Zvi 1987). When the probability distribution of the cumulated discharge is skewed, the use of a logarithmic transformation can help to approach the normal distribution. Hence, Nalbantis and Tsakiris (2009) addressed

Table 2. Performance of SWAT model during calibration and validation stages

Statistics	Neches River Basin		Trinity River Basin	
	Calibration (1991–1995)	Validation (1996–2015)	Calibration (1991–1995)	Validation (1996–2015)
Nash-Sutcliffe efficiency (NSE)	0.65	0.62	0.64	0.56
Index of agreement, d	0.92	0.86	0.86	0.79
RMS error [RMSE (m^3/s)]	103.65	118.65	147.97	146.46

streamflow drought using a logarithmic transformation of cumulative discharge data

$$\mathrm{SDI}_{\tau,\theta} = \frac{y_{\tau,\theta} - \bar{y}_{\tau,\theta}}{s_{\tau,\theta}}; \quad \tau = 1, 2, \ldots, n; \quad \theta = 1, 2, 3, 4 \quad (7)$$

$$y_{\tau,\theta} = \ln(V_{\tau,\theta}); \quad \tau = 1, 2, \ldots, n; \quad \theta = 1, 2, 3, 4 \quad (8)$$

In general, the shape of a watershed can influence the empirical probability distribution of the discharge data (Kroll and Vogel 2002). Subsequently, the use of a standard probability distribution is not straightforward. For small watersheds, the probability distribution of the cumulative discharge is often skewed and approximate to the gamma distribution family (Nalbantis and Tsakiris 2009; Ben-Zvi 1987). In such cases, the data can be transformed to fit a normal distribution. In this study, a logarithmic transformation of the cumulative discharge data was found necessary following a goodness-of-fit analysis. The goodness-of-fit analysis was separately conducted for both observed and simulated cumulated discharge data of individual watershed. The gamma [Eq. (9)] and lognormal [Eq. (10)] probability density function (PDF) parameters were estimated and reported

$$f_{(V)} = \frac{1}{\beta^{\alpha}\Gamma_{(\alpha)}} V^{\alpha-1} e^{-V/\beta} \quad (9)$$

$$f_{(y)} = \frac{1}{\sigma_y\sqrt{2\pi}} \exp\left[-\frac{1}{2}\left(\frac{y-\mu_y}{\sigma_y}\right)^2\right] \quad \text{where } y = \ln(V) \quad (10)$$

where V = cumulative discharge value; $y = \ln(V)$ = natural logarithm of V; μ_y and σ_y = mean and variance of y, respectively; α and β = shape parameter and scale parameter, respectively, of the gamma PDF, where $\alpha > 0$ and $\beta > 0$; $V > 0$ satisfies the condition of the gamma distribution; and $\text{mean}(V) = \alpha \times \beta$ and variance $(V) = \alpha \times \beta^2$.

The goodness-of-fit analysis was conducted using the Kolmogorov-Smirnov (K-S) test. The Kolmogorov-Smirnov test for goodness-of-fit is performed to evaluate how closely the empirical cumulative discharge data and the transformation follow each of the theoretical probability density functions, namely the gamma and lognormal PDF (Vicente-Serrano et al. 2012). The Kolmogorov-Smirnov test statistic, D, is

$$D = \max\{|F(x) - G(x)|\} \quad (11)$$

where F = theoretical cumulative distribution function; and G = empirical probability distribution of the cumulative discharge being tested. The calculated D value is compared with a critical value. At p-value = 0.05, the critical value of D is given by $D_{\text{critical}} = 1.358 \times N^{-0.5}$, where N represents the size of the tested sample. If $D_{\text{calculated}} < D_{\text{critical}}$, the sample data are assumed to be a good fit with the theoretical distribution; otherwise, the null hypothesis of a good fit is rejected (Lopes 2011).

Results

Performance of SWAT Model

The delineated watershed in the Neches River Basin expands over a spatial domain of 19,574 km^2, whereas the one in the Trinity River Basin covers 33,262 km^2. In the Neches River Basin, a total of 209 subbasins and 11,374 hydrologic response units (HRUs) were identified during the SWAT modeling process. Similarly, 391 subbasins and 12,485 HRUs were identified in the Trinity River Basin. The SWAT calibration was successfully conducted using the period of 1990–1995, but the year 1990 was considered as a warming period. Hence, the performance indicators were only computed for the simulated period 1991–1995 (i.e., October 1990–September 1995). The performance of the calibrated SWAT model is reported in Table 2. The NSE was 0.65 for the Neches watershed, and the NSE was 0.64 for Trinity. The calibrated SWAT model was later validated using a 2-decade time frame (i.e., October 1995–September 2015). The overall performance of the model at this stage is depicted in Fig. 3. Although peak discharges were overpredicted during certain years of the validation period, the overall performance of the SWAT model was acceptable based on the efficiency indicators reported in Table 2 (NSE = 0.62 for Neches and NSE = 0.56 for Trinity). The values of the calculated index of agreement d and RMSE (Table 2) also confirmed the consistency of the calibration and validation.

Streamflow Drought Assessment

The procedure developed for the streamflow drought assessment included three steps. The first step consisted of the goodness-of-fit test of gamma and lognormal distributions of observed and simulated cumulative discharge data. This step is reported to show that the cumulative discharge data were skewed and needed a normal approximation in order to apply SDI (Ben-Zvi 1987). The second step was the computation of SDI time series for past and future periods, and the third step was the comparative analysis of SDI signals.

Goodness-of-Fit Analysis of Streamflow Data

The goodness-of-fit analysis was conducted separately for the observed and simulated data (i.e., cumulative discharge), using the Kolmogorov-Smirnov test. The K-S test was carried out distinctly for the Neches and the Trinity watersheds. The results of the K-S test for the observed data (period 1996–2015) and the simulated data (periods 1996–2015 and 2041–2070), are reported in Table 3 and portrayed in Fig. 4. The outcomes of the K-S tests indicated that the raw cumulative streamflow (observed and simulated) initially fit the family of gamma distribution functions (Table 3). Hence, to use the SDI Eqs. (4)–(6), it was important to transform the cumulative discharge probability distribution into a normal distribution (Ben-Zvi 1987). The results in Table 3 and Fig. 4 show that the logarithmic transformation of the data can help to approximate the theoretical normal distribution. Hence, the study used the

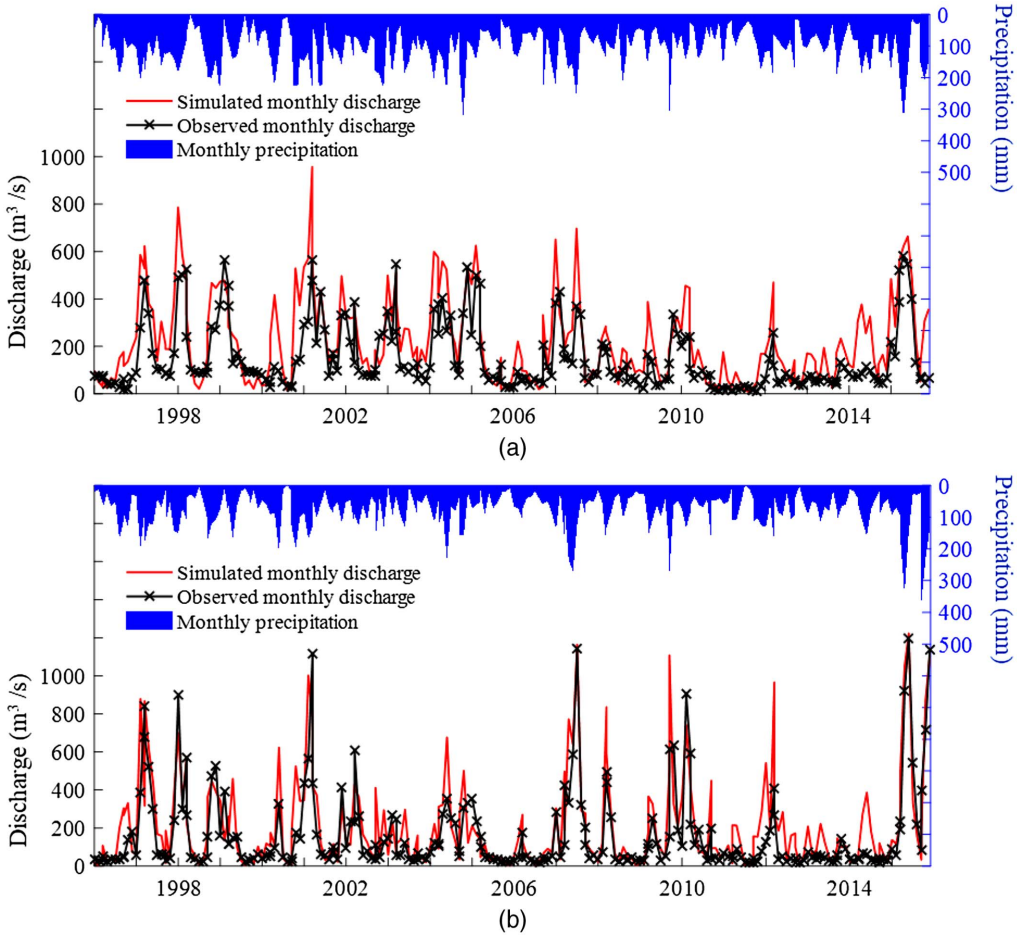

Fig. 3. Validation of SWAT model simulation of two-decade monthly discharge in the (a) Neches River Basin; and (b) Trinity River Basin.

Table 3. Goodness-of-fit analysis of observed and SWAT-simulated discharges in Neches and Trinity watersheds with gamma and lognormal theoretical distributions using Kolmogorov-Smirnov test

		Gamma distribution			Lognormal distribution		
Watershed	Discharge data	α	β	K-S test (D)	μ_y	σ_y	K-S test (D)
Neches	Observed (1996–2015)	1.26	2,046.08	0.07[a]	7.30	1.22	0.11[a]
	Simulated (1996–2015)	1.49	2,584.78	0.08[a]	7.74	1.22	0.15[a]
	Simulated (2041–2070)	0.81	4,175.93	0.09[a]	7.32	1.53	0.07[a]
Trinity	Observed (1996–2015)	1.01	2,642.76	0.10[a]	7.25	1.29	0.10[a]
	Simulated (1996–2015)	1.28	2,749.79	0.06[a]	7.61	1.23	0.14[a]
	Simulated (2041–2070)	0.88	7,694.12	0.10[a]	7.98	1.62	0.11[a]

Note: Estimated parameters of gamma and lognormal PDFs are reported. The critical value of D is given by $D_{0.95} = 1.358N^{-0.5}$, where N is the sample size (for the test, $N = 40$ and $D_{0.95} = 0.21$).
[a]Calculated D value is below the critical value at p-value = 0.05, meaning the null hypothesis cannot be rejected.

lognormal distribution for the SDI estimate. These results are consistent with those reported by Nalbantis and Tsakiris (2009) who also used the lognormal distribution to estimate SDI. Ultimately, Eqs. (7) and (8) were included in the calculation of SDI time series in both watersheds.

SDI Signals Captured by SWAT Model

Fig. 5 portrays the performance of the SWAT model in reproducing signals of streamflow drought. The plotted SDI time series were estimated based on the observed streamflow and the SWAT model simulated flow for period 1996–2015. The SDI values were estimated distinctly for the Neches and Trinity watersheds using the procedure described in subsection "Streamflow Drought Index." In addition, the computation of SDI was carried out separately for the reference periods of the hydrological year, namely $\theta = 1$ (October–December), $\theta = 2$ (October–March), $\theta = 3$ (October–June), and $\theta = 4$ (October–September). For each of these reference periods, Table 4 reports significant correlations between the SDI values retrieved from observed discharges and those estimated from SWAT simulations. This pattern is sustained by Fig. 5, which show the time series of SDI of observed and simulated discharges for each reference period. The gaps between the SDI of observed and simulated discharges varied depending on the watershed and the reference period of the hydrologic year. The SWAT model

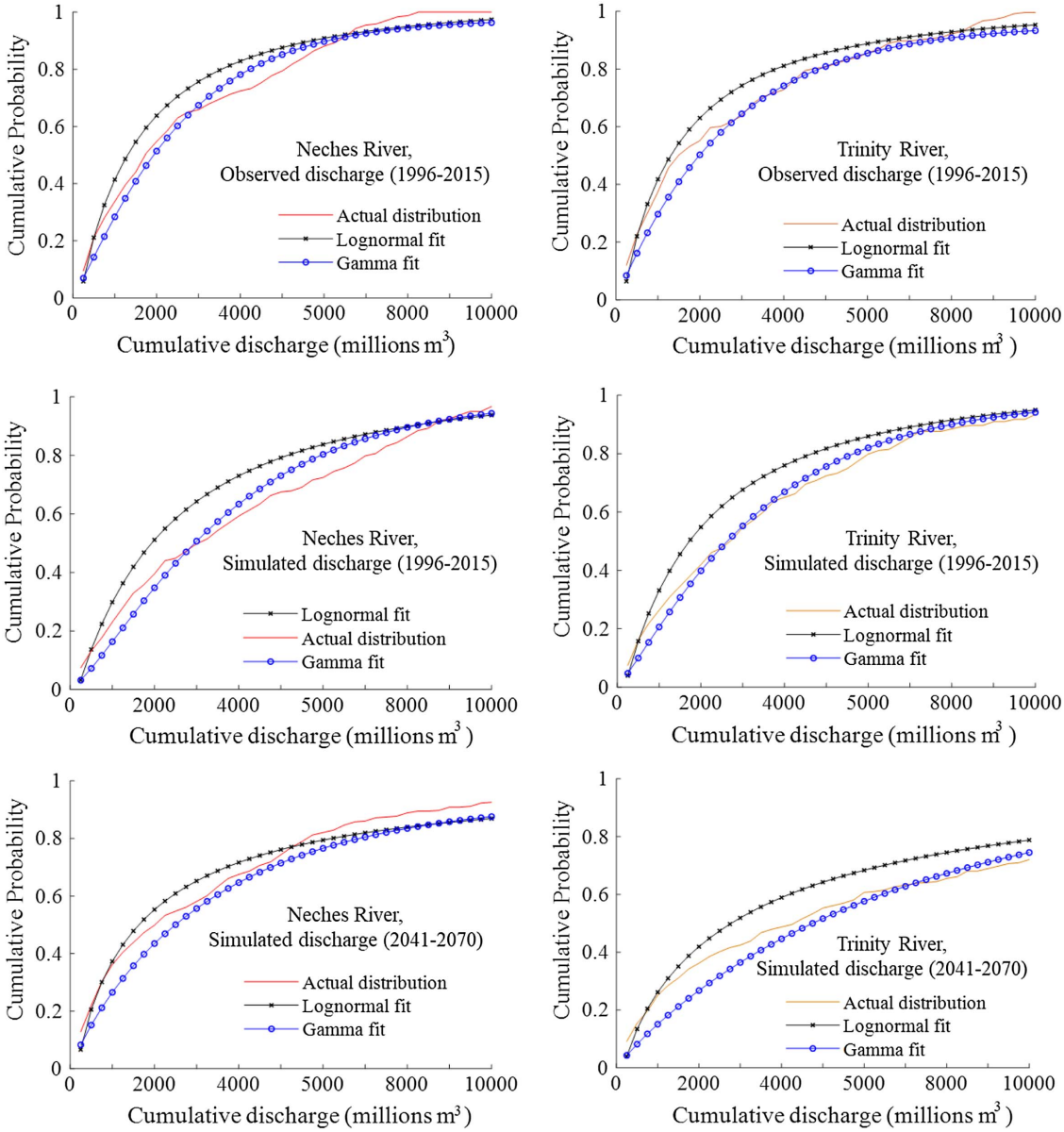

Fig. 4. Fitting the empirical cumulative probability distribution of observed and simulated cumulative streamflow data with the expected gamma and lognormal cumulative probability distributions.

captured 52%–91% ($0.52 \leq R^2 \leq 0.91$) of SDI variance in the Neches watershed, and 79%–89% ($0.79 \leq R^2 \leq 0.89$) of SDI variance in the Trinity watershed (Table 4). Interestingly, these values of R^2 obtained with SDI analysis are high, and this suggests that the SWAT model captures more closely the streamflow drought signals. As a result, the use of SWAT model simulation for SDI projections may turn to be a robust estimate of streamflow patterns at the watershed scale.

Analysis of Future Streamflow Drought Patterns

As mentioned previously, the calibrated SWAT model was used to simulate future streamflow (i.e., 2041–2070). The simulation used data of future climate scenario projected by the NARCCAP RCM3-GFDL (Wehner 2013) for weather inputs. As indicated in section "Goodness-of-Fit Analysis of Streamflow Data" (Table 3), the probability density of the cumulative discharge (simulated data) for the period 2041–2070 can be fitted to a theoretical lognormal function to enable the SDI computation. Eqs. (7) and (8) were therefore considered in the calculation of the corresponding SDI values. This subsection evaluates how much the future patterns of streamflow drought departed from the past patterns in each watershed (i.e., Neches and Trinity). The SDI values for future and past periods (2041–2070 and 1996–2015) were classified within the five categories of streamflow drought. The resulting histograms of frequencies of SDI corresponding to the reference periods (i.e., $\theta = 1$ = October–December, $\theta = 2$ = October–March, $\theta = 3$ = October–June, and $\theta = 4$ = October–September) are presented in Fig. 6. This analysis is complemented with a χ^2 statistic test of homogeneity which evaluated how well the distribution of SDI during the future period 2041–2070 reflects the past period 1996–2015 (Bangdiwala 2016; Franke et al. 2012). Specifically, the χ^2 statistic tested the null hypothesis H_0 that the distributions of SDI within the five categories of streamflow drought [i.e., no drought ($0 \leq$ SDI), mild ($-1 \leq$ SDI < 0), moderate ($-1.5 \leq$ SDI < -1), severe ($-2 \leq$ SDI < -1.5), and extreme (SDI < -2)] were

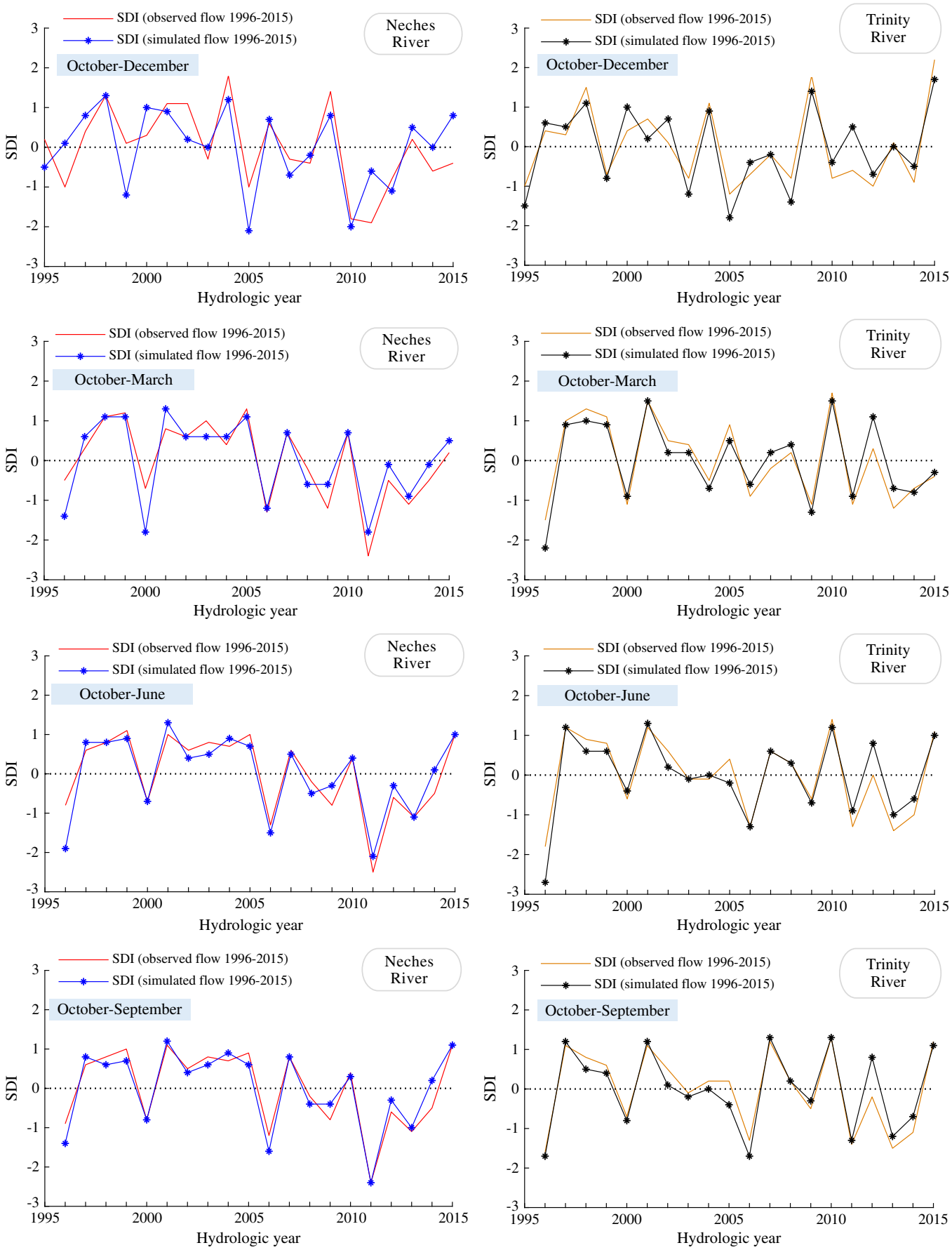

Fig. 5. Time series of SDI derived from observed cumulative discharge compared with those derived from SWAT model simulations during the period 1996–2015.

Table 4. Estimating the correlations between observed SDI and SWAT simulated SDI over period 1996–2015 for different referential periods of hydrological year

Referential period of hydrological year	Sample size	Coefficient of determination R^2	
		Neches River	Trinity River
$\theta = 1$ (October–December)	21	0.52	0.79
$\theta = 2$ (October–March)	20	0.81	0.89
$\theta = 3$ (October–June)	20	0.87	0.87
$\theta = 4$ (October–September)	20	0.91	0.89

identical during the future period 2041–2070 and the past period 1996–2015. The calculation frame for the χ^2 statistic is reported in Table 5 which drew the absolute frequencies of drought categories. The statistic value $\chi^2_{\text{calculated}}$ is calculated using

$$\chi^2_{\text{calculated}} = \sum_{\lambda=1}^{2}\sum_{\rho=1}^{5}\frac{(X_{\lambda,\rho} - X_{\lambda,.}X_{.,\rho}/X_{...})^2}{X_{\lambda,.}X_{.,\rho}/X_{...}} \quad \text{with df} = 4 \quad (12)$$

where df = degrees of freedom; λ indicates period, where $\lambda = 1$ = 1996–2015 and $\lambda = 2$ = 2041–2070); ρ indicates SDI categories (Table 5); and X represents absolute frequencies.

The critical value χ^2_α at p-value = 0.05 and df = 4 is equal to 9.49 [i.e., $\chi^2_{0.05}(\text{df} = 4) = 9.49$]. The calculated statistics are $\chi^2_{\text{calculated}} = 3.24$ in the Neches watershed and $\chi^2_{\text{calculated}} = 5.32$ in the Trinity watershed. In both cases, $\chi^2_{\text{calculated}} < \chi^2_\alpha$, and thus we did not reject the hypothesis H_0. This means that the future patterns of streamflow drought in each watershed will likely be similar to those observed in the past. However, the inferences driven in this analysis are based on assumptions associated with the NARCCAP RCM3-GFDL simulation. Probably, different results would be observed if a different climate scenario were assumed. Nevertheless, this estimate of SDI using climate model outputs is relevant and useful to get insight into surface water resources availability under the imminent fact of climate disturbance (Chattopadhyay et al. 2017; Bucak et al. 2017).

Discussion

This study evaluated how well the SWAT model captures streamflow drought pattern over a long run (multiple decades). Two watersheds, namely the Neches and Trinity River Basins, were considered and simulated separately. The SWAT model was calibrated using monthly discharge time series of 1990–1995. Thereafter, the calibrated model was used to simulate monthly discharge for past period 1996–2015 (validation) and future period 2041–2070. Although the accuracy of the SWAT simulation is highly dependent on the quality of the input data, there is no perfect model simulation (Gassman et al. 2014; Mukundan et al. 2010; Geza and McCray 2008). An evaluation of the SWAT model performance based on efficiency criteria (i.e., NSE and index of agreement d) indicated acceptable simulations during both calibration and validation periods. The simulations of the future period 2041–2070 are a probable representation of the future flow even though there are limitations associated with the inputs used in the future scenario simulations (i.e., the NLCD 2011 used as default input for land-cover data, and the uncertainties associated with the NARCCAP RCM3-GFDL inputs).

Following the SWAT model simulation, SDI values were estimated for both observed and simulated discharges. However, the SDI formulation used in the study requires a knowledge of the probability distribution of the cumulative discharge. The SDI computation reported by Nalbantis and Tsakiris (2009) is applicable when the PDF of cumulative discharge is normal or transformed into a normal distribution. When the cumulated discharge probability is skewed (e.g., gamma distributed), a normal transformation is needed before applying SDI (Nalbantis and Tsakiris 2009; Ben-Zvi 1987). The Kolmogorov-Smirnov's goodness-of-fit analysis conducted on both observed and simulated data suggested a fitting of the cumulative discharge to the lognormal distribution for SDI application (Nalbantis and Tsakiris 2009). The logarithmic transformation of the observed and simulated discharge data was then used to estimate SDI values in each watershed. The SDI values were computed for each of the reference periods (i.e., $\theta = 1$ = October–December, $\theta = 2$ = October–March, $\theta = 3$ = October–June, and $\theta = 4$ = October–September). Interestingly, for the period 1996–2015, the SDI time series derived distinctly from the observed discharge were closely analogous to the SDI estimated based on the SWAT simulation for the same period (Fig. 5 and Table 4). However, the accuracy of the SWAT simulations' SDI seems to depend on the watershed and the reference period of the hydrologic year (Table 4). This disparity could be, in part, attributed to the difference of efficiency during the SWAT simulation (NSE = 0.62 for Neches, and NSE = 0.56 for Trinity). Regardless of these variations, the overall results obtained for the period 1996–2015 demonstrated the capacity of the SWAT model to capture and closely reproduce streamflow drought signals over a multidecadal time frame. Therefore, the SWAT model simulations of discharge for period 2041–2070 were considered for projecting future patterns of SDI in the Neches and the Trinity watersheds.

Even though a visual analysis of the histograms in Fig. 6 may suggest slight differences, the frequency distributions of projected SDI for the period 2041–2070 were found to be statistically homogeneous to the distributions of SDI for the past period 1996–2015. The physical meaning of this statistical result is that the two watersheds are likely to experience similar patterns of streamflow in the future. However, this inference is based on the assumptions associated with the inputs used during the SWAT modeling process. These assumptions are notably related to the NARCCAP RCM3-GFDL and the land-cover input, which was assumed to be the same as that of NLCD 2011. Regardless of these shortcomings, a similarity of SDI patterns between past and future periods may not imply systematically that the water resources will be sufficient to satisfy societal needs in the future. For instance, given the actual growth rate of the population, freshwater demand is expected to increase consequently in both watersheds. Hence, the project SDI pattern is probably an early warning for freshwater security at the watershed scale. This is true because the quantitative availability of streamflow in a watershed is vital for natural ecosystems and human society as well (Poff et al. 1997).

A watershed represents a physical interface in which animals, plants, and humans live, interact, and share the same water resources (Tidwell et al. 2004; Montgomery et al. 1995). As a major component of surface water, the regime of streamflow is likely to reflect the biophysical functionality of a watershed (Sohoulande Djebou and Singh 2016; Sohoulande Djebou 2015). Interannual and intra-annual variability of streamflow regimes are inherent to natural watersheds, but the scientific understanding of this variability is useful for decision-making in water resources and environment management (Sohoulande Djebou 2018; Montgomery et al. 1995). In the case of the Neches and Trinity watersheds, the observed signals of SDI indicate that the lower categories of streamflow drought are dominant. However, this overall dominance should not rule out the alert related to severe streamflow drought episodes

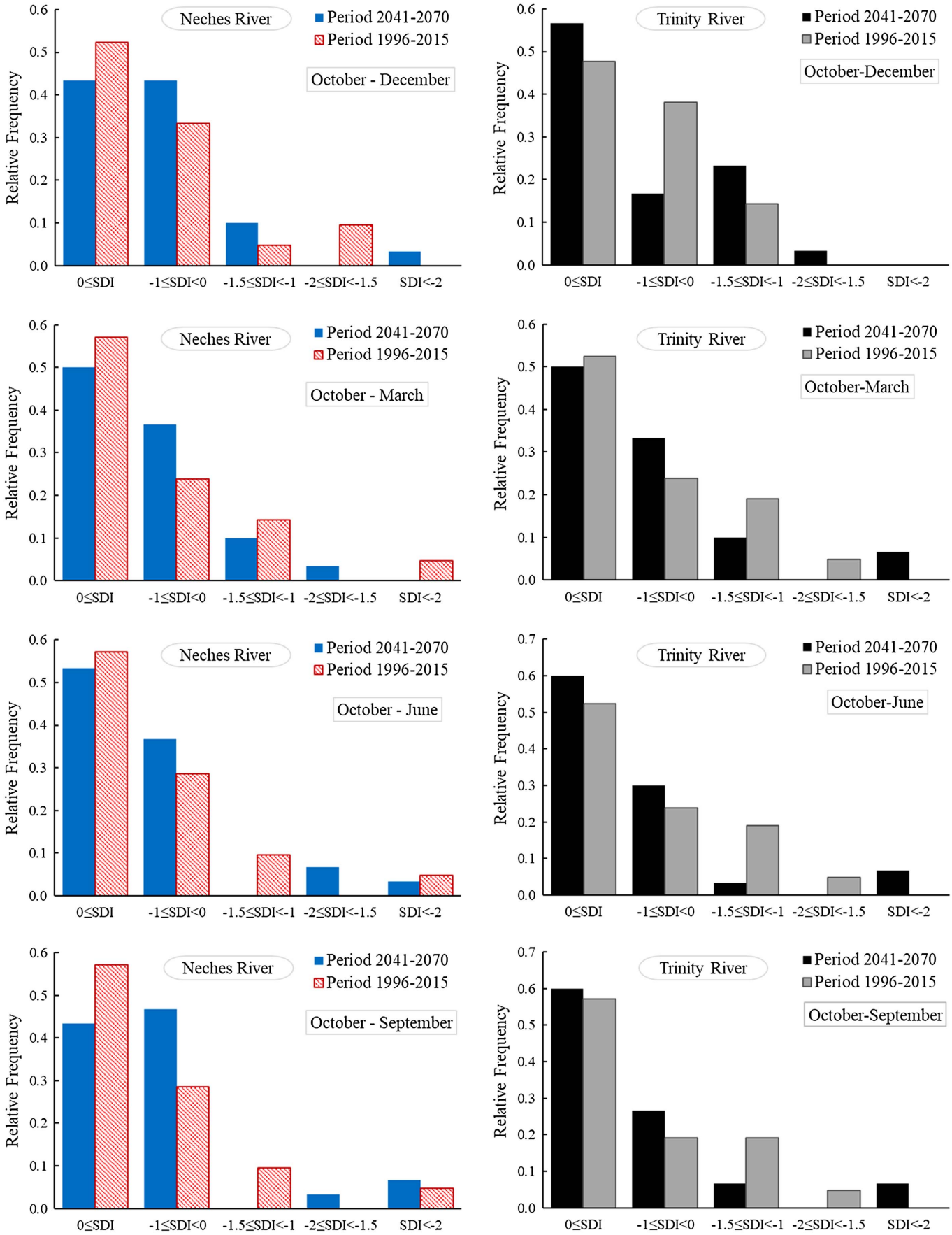

Fig. 6. Frequencies of streamflow drought categories during the past (1996–2015) and future (2041–2070) periods. The streamflow drought index SDI of the future period were estimated based on SWAT model simulations. Cumulative discharges for October–December, October–March, October–June, and October–September were analyzed separately.

Table 5. Scheme of table of frequency used for calculation of $\chi^2_{\text{calculated}}$

Drought category	Absolute frequencies		Total
	Past scenario (1996–2015)	Future scenario (2041–2070)	
No drought ($0 \leq$ SDI)	$X_{1,1}$	$X_{2,1}$	$X_{.,1} = X_{1,1} + X_{2,1}$
Mild ($-1 \leq$ SDI < 0)	$X_{1,2}$	$X_{2,2}$	$X_{.,2} = X_{1,2} + X_{2,2}$
Moderate ($-1.5 \leq$ SDI < -1)	$X_{1,3}$	$X_{2,3}$	$X_{.,3} = X_{1,3} + X_{2,3}$
Severe ($-2 \leq$ SDI < -1.5)	$X_{1,4}$	$X_{2,4}$	$X_{.,4} = X_{1,4} + X_{2,4}$
Extreme (SDI < -2)	$X_{1,5}$	$X_{2,5}$	$X_{.,5} = X_{1,5} + X_{2,5}$
Total	$X_{1,.} = X_{1,1} + X_{1,2} + X_{1,3} + X_{1,4} + X_{1,5}$	$X_{2,.} = X_{2,1} + X_{2,2} + X_{2,3} + X_{2,4} + X_{2,5}$	$X_{.,.} = X_{1,.} + X_{2,.}$

which can be costly for the environment and society (Smakhtin 2001; Montgomery et al. 1995).

Conclusion

In water resources planning, the streamflow drought index SDI is very useful because it allows a probabilistic interpretation of flow fluctuation in time and space (Tabari et al. 2013). With the ongoing trend of freshwater depletion, a projection of SDI is needed to sustain water resources planning on the long-term. This paper reported a case study which used SWAT model simulations to estimate SDI for past and future periods. It was found that the SWAT model simulations captured sufficiently the variance of SDI during the different periods of the hydrologic year. The capacity of SWAT to closely reproduce streamflow drought signals over a multidecadal period was also outlined. Hence, it is concluded that the SWAT model could be considered to project SDI patterns at the watershed level. However, the projections are dependent on the climate scenario included in the SWAT simulations. Thus, the interpretation of the future SDI patterns described in this paper must consider the assumptions related to the NARCCAP future climate data incorporated into the SWAT model simulations.

Acknowledgments

The author acknowledges the different institutions which released the data used in the study, including the USGS, the NOAA, the USDA, and the USEPA. The author acknowledges the Spatial Sciences Laboratory at Texas A&M Univ. for the technical support received during SWAT modeling. The author also thanks the anonymous reviewers for their useful assessments.

Disclaimer

Mention of trade names or commercial products in this article is solely for the purpose of providing specific information and does not imply recommendation or endorsement by the US Department of Agriculture.

References

Ahmed, K. F., G. Wang, J. Silander, A. M. Wilson, J. M. Allen, R. Horton, and R. Anyah. 2013. "Statistical downscaling and bias correction of climate model outputs for climate change impact assessment in the U.S. northeast." *Global Planet. Change* 100 (Jan): 320–332. https://doi.org/10.1016/j.gloplacha.2012.11.003.

Bangdiwala, S. I. 2016. "Chi-squared statistics of association and homogeneity." *Int. J. Inj. Control Saf. Promotion* 23 (4): 444–446. https://doi.org/10.1080/17457300.2016.1228144.

Ben-Zvi, A. 1987. "Indices of hydrological drought in Israel." *J. Hydrol.* 92 (1–2): 179–191. https://doi.org/10.1016/0022-1694(87)90095-3.

Bucak, T., D. Trolle, H. E. Andersen, H. Thodsen, Ş. Erdoğan, E. E. Levi, N. Filiz, E. Jeppesen, and M. Beklioğlu. 2017. "Future water availability in the largest freshwater Mediterranean lake is at great risk as evidenced from simulations with the SWAT model." *Sci. Total Environ.* 581 (Mar): 413–425. https://doi.org/10.1016/j.scitotenv.2016.12.149.

Chattopadhyay, S., D. R. Edwards, Y. Yu, and A. Hamidisepehr. 2017. "An assessment of climate change impacts on future water availability and droughts in the Kentucky River Basin." *Environ. Process.* 4 (3): 477–507. https://doi.org/10.1007/s40710-017-0259-2.

Deo, R. C., O. Kisi, and V. P. Singh. 2017. "Drought forecasting in eastern Australia using multivariate adaptive regression spline, least square support vector machine and M5Tree model." *Atmos. Res.* 184 (Feb): 149–175. https://doi.org/10.1016/j.atmosres.2016.10.004.

Eckhardt, K., and J. G. Arnold. 2001. "Automatic calibration of a distributed catchment model." *J. Hydrol.* 251 (1–2): 103–109. https://doi.org/10.1016/S0022-1694(01)00429-2.

Franke, T. M., T. Ho, and C. A. Christie. 2012. "The chi-square test: Often used and more often misinterpreted." *Am. J. Eval.* 33 (3): 448–458. https://doi.org/10.1177/1098214011426594.

Gassman, P. W., A. M. Sadeghi, and R. Srinivasan. 2014. "Applications of the SWAT model special section: Overview and insights." *J. Environ. Qual.* 43 (1): 1–8. https://doi.org/10.2134/jeq2013.11.0466.

Geza, M., and J. E. McCray. 2008. "Effects of soil data resolution on SWAT model stream flow and water quality predictions." *J. Environ. Manage.* 88 (3): 393–406. https://doi.org/10.1016/j.jenvman.2007.03.016.

Homer, C. G., J. A. Dewitz, L. Yang, S. Jin, P. Danielson, G. Xian, J. Coulston, N. D. Herold, J. D. Wickham, and K. Megown. 2015. "Completion of the 2011 National Land Cover Database for the conterminous United States—Representing a decade of land cover change information." *Photogramm. Eng. Remote Sens.* 81 (5): 345–354. https://doi.org/10.1016/S0099-1112(15)30100-2.

Kroll, C. N., and R. M. Vogel. 2002. "Probability distribution of low streamflow series in the United States." *J. Hydrol. Eng.* 7 (2): 137–146. https://doi.org/10.1061/(ASCE)1084-0699(2002)7:2(137).

Legates, D. R., and G. J. McCabe Jr. 1999. "Evaluating the use of 'goodness-of-fit' measures in hydrologic and hydroclimatic model validation." *Water Res.* 35 (1): 233–241. https://doi.org/10.1029/1998WR900018.

Lopes, R. H. 2011. "Kolmogorov-Smirnov test." In *International encyclopedia of statistical science*, 718–720. Berlin: Springer.

McCuen, R. H., Z. Knight, and A. G. Cutter. 2006. "Evaluation of the Nash-Sutcliffe efficiency index." *J. Hydrol. Eng.* 11 (6): 597–602. https://doi.org/10.1061/(ASCE)1084-0699(2006)11:6(597).

McKee, T. B., N. J. Doesken, and J. Kleist. 1993. "The relationship of drought frequency and duration to time scales." In Vol. 17 of *Proc., 8th Conf. on Applied Climatology*, 179–183. Boston: American Meteorological Society.

Mearns, L. O., et al. 2012. "The North American regional climate change assessment program overview of Phase I results." *Bull. Am. Meteorol. Soc.* 93 (9): 1337–1362. https://doi.org/10.1175/BAMS-D-11-00223.1.

Mishra, A. K., and V. R. Desai. 2006. "Drought forecasting using feed-forward recursive neural network." *Ecol. Modell.* 198 (1): 127–138. https://doi.org/10.1016/j.ecolmodel.2006.04.017.

Montgomery, D. R., G. E. Grant, and K. Sullivan. 1995. "Watershed analysis as a framework for implementing ecosystem management." *J. Am. Water Resour. Assoc.* 31 (3): 369–386. https://doi.org/10.1111/j.1752-1688.1995.tb04026.x.

Mukundan, R., D. E. Radcliffe, and L. M. Risse. 2010. "Spatial resolution of soil data and channel erosion effects on SWAT model predictions of flow and sediment." *J. Soil Water Conserv.* 65 (2): 92–104. https://doi.org/10.2489/jswc.65.2.92.

Nakicenovic, N., J. Alcamo, G. Davis, B. De Vries, J. Fenhann, S. Gaffin, K. Gregory, A. Grübler, T. Y. Jung, and T. Kram. 2000. *Special report on emissions scenarios: A special report of Working Group III of the Intergovernmental Panel on Climate Change*, 599. Cambridge, UK: Cambridge University Press.

Nalbantis, I., and G. Tsakiris. 2009. "Assessment of hydrological drought revisited." *Water Resour. Manage.* 23 (5): 881–897. https://doi.org/10.1007/s11269-008-9305-1.

Poff, N. L., J. D. Allan, M. B. Bain, J. R. Karr, K. L. Prestegaard, B. D. Richter, R. E. Sparks, and J. C. Stromberg. 1997. "The natural flow regime." *BioScience* 47 (11): 769–784. https://doi.org/10.2307/1313099.

Slack, J. R., and J. M. Landwehr. 1992. *Hydro-climatic data network (HCDN); a US Geological Survey streamflow data set for the United States for the study of climate variations*. Open-File Reports Section. No. 92-129. Washington, DC: USGS.

Smakhtin, V. U. 2001. "Low flow hydrology: A review." *J. Hydrol.* 240 (3): 147–186. https://doi.org/10.1016/S0022-1694(00)00340-1.

Sohoulande Djebou, D. C. 2015. "Integrated approach to assessing streamflow and precipitation alterations under environmental change: Application in the Niger River Basin." *J. Hydrol. Reg. Stud.* 4 (Sep): 571–582. https://doi.org/10.1016/j.ejrh.2015.09.004.

Sohoulande Djebou, D. C. 2017. "Bridging drought and climate aridity." *J. Arid Environ.* 144 (Sep): 170–180. https://doi.org/10.1016/j.jaridenv.2017.05.002.

Sohoulande Djebou, D. C. 2018. "Toward an integrated watershed zoning framework based on the spatio-temporal variability of land-cover and climate: Application in the Volta river basin." *Environ. Dev.* 28 (Dec): 55–66. https://doi.org/10.1016/j.envdev.2018.09.006.

Sohoulande Djebou, D. C., and V. P. Singh. 2016. "Entropy-based index for spatiotemporal analysis of streamflow, precipitation, and land-cover." *J. Hydrol. Eng.* 21 (11): 05016024. https://doi.org/10.1061/(ASCE)HE.1943-5584.0001429.

Tabari, H., J. Nikbakht, and P. H. Talaee. 2013. "Hydrological drought assessment in Northwestern Iran based on streamflow drought index (SDI)." *Water Resour. Manage.* 27 (1): 137–151. https://doi.org/10.1007/s11269-012-0173-3.

Tidwell, V. C., H. D. Passell, S. H. Conrad, and R. P. Thomas. 2004. "System dynamics modeling for community-based water planning: Application to the Middle Rio Grande." In Vol. 66 of *Aquatic sciences*, 357–372. New York: New York Academy of Sciences.

Vicente-Serrano, S. M., J. I. López-Moreno, S. Beguería, J. Lorenzo-Lacruz, C. Azorin-Molina, and E. Morán-Tejeda. 2012. "Accurate computation of a streamflow drought index." *J. Hydrol. Eng.* 17 (2): 318–332. https://doi.org/10.1061/(ASCE)HE.1943-5584.0000433.

Vrugt, J. A., C. J. F. ter Braak, M. P. Clark, J. M. Hyman, and B. A. Robinson. 2008. "Treatment of input uncertainty in hydrologic modeling: Doing hydrology backward with Markov chain Monte Carlo simulation." *Water Resour. Res.* 44 (12): 1–15. https://doi.org/10.1029/2007WR006720.

Wang, X., and A. M. Melesse. 2006. "Effects of STATSGO and SSURGO as inputs on SWAT model's snowmelt simulation." *J. Am. Water Resour. Assoc.* 42 (5): 1217–1236. https://doi.org/10.1111/j.1752-1688.2006.tb05296.x.

Wehner, M. F. 2013. "Very extreme seasonal precipitation in the NARCCAP ensemble: Model performance and projections." *Clim. Dyn.* 40 (1–2): 59–80. https://doi.org/10.1007/s00382-012-1393-1.

Wilhite, D. A., and M. H. Glantz. 1985. "Understanding: The drought phenomenon: The role of definitions." *Water Int.* 10 (3): 111–120. https://doi.org/10.1080/02508068508686328.

Willmott, C. J. 1981. "On the validation of models." *Phys. Geogr.* 2 (2): 184–194. https://doi.org/10.1080/02723646.1981.10642213.

Zabaleta, A., M. Meaurio, E. Ruiz, and I. Antigüedad. 2014. "Simulation climate change impact on runoff and sediment yield in a small watershed in the Basque Country, northern Spain." *J. Environ. Qual.* 43 (1): 235–245. https://doi.org/10.2134/jeq2012.0209.